Supplementary figure 1 Mean and 95 percent normal probability interval of each symptom in each class of the model with 5 classes (4 genetic classes and 1 non-genetic class) and within-class standard deviation $\sigma = 15$.

Supplementary figure 2 Distribution of the number of classes inferred by the likelihood cross-validation procedure in 400 replications. Boxes indicate the actual number of classes, σ is the within-class standard deviation.

Supplementary figure 3 Power to detect association to a DS variant with a marker perfectly correlated ($r^2 = 1$) in simulations of an heterogeneity model with four DS variants (4G5C model). Datasets contain 400 families with two affected siblings and parents with no phenotypic information. Genotypes of all family members are observed. For LC-derived phenotypes, p-values were multiplied by the number of classes. The significance level was set to 5×10^{-8}. Results are based on 400 replicates. Panel A shows the results of an analysis under the dominant model, panel B, D and E results under the additive model and panel C results under the recessive model. Error bars represent exact 95% confidence intervals. The first four bars from the left on each panel represent power using LC-derived phenotypes: P: posterior probability of class membership used as a quantitative trait in affected subjects, C: most probable class used as phenotype, σ: within-class standard deviation. The rightmost bar (orig) represents power using the original phenotype where all symptomatic subjects are affected.

Supplementary figure 4 Power to detect association to a DS variant with a marker correlated at $r^2 = 0.8$ in simulations of an heterogeneity model with two DS variants (2G3C model). Datasets contain 150 families with two affected siblings and parents with no phenotypic information. Genotypes of all family members are observed. For LC-derived phenotypes, p-values were multiplied by the number of classes. The significance level was set to 5×10^{-8}. Results are based on 400 replicates. Panel A shows the results of an analysis under the dominant model, panel B and D results under the additive model and panel C results under the recessive model. Error bars represent exact 95% confidence intervals. The

first four bars from the left on each panel represent power using LC-derived phenotypes: P: posterior probability of class membership used as a quantitative trait in affected subjects, C: most probable class used as phenotype, σ: within-class standard deviation. The rightmost bar (orig) represents power using the original phenotype where all symptomatic subjects are affected.

Supplementary figure 5 Power to detect association to a DS variant with a marker perfectly correlated ($r^2 = 1.0$) in simulations of an heterogeneity model with two DS variants (2G3C model). Datasets contain 150 families with two affected siblings and parents with no phenotypic information. Genotypes of all family members are observed. For LC-derived phenotypes, p-values were multiplied by the number of classes. The significance level was set to 5×10^{-8}. For LC-derived phenotypes, this significance level was divided by the number of classes. Results are based on 400 replicates. Panel A shows the results of an analysis under the dominant model, panel B and D results under the additive model and panel C results under the recessive model. Error bars represent exact 95% confidence intervals. The first four bars from the left on each panel represent power using LC-derived phenotypes: P: posterior probability of class membership used as a quantitative trait in affected subjects, C: most probable class used as phenotype, σ: within-class standard deviation. The rightmost bar (orig) represents power using the original phenotype where all symptomatic subjects are affected.

Supplementary figure 6 Absolute Z score against absolute difference between the score S and its expectation, $S - E[S]$, for markers correlated at $r^2 = 0.8$ and $r^2 = 1.0$ with the recessive DS variant. Each dot represents one of the 400 replicates. $S - E[S]$ is an indication of the number of informative transmissions. For a fixed $S - E[S]$, the recessive model gives larger Z scores than the additive model, as expected. This advantage is however reduced by genotype misclassification when using a marker at $r^2 = 0.8$ compared to the actual DS variant, likely because a change from a heterozygous to an homozygous genotype in one of the two parents makes the whole family uninformative under the recessive model, while the transmission from the remaining heterozygous parent remains informative under

the additive model. At the same time, the number of informative transmissions tends to be larger under the additive model, and at $r^2 = 0.8$ the combined effect of genotype misclassification and larger number of informative transmissions leads to larger Z scores under the additive than the recessive model, since the magnitude of the Z score is positively associated to the number of informative transmissions. With the original affection status, inclusion of subjects in other classes leads to a larger variance and lower Z scores for a fixed value of $S - E[S]$, and more so under the additive than the recessive model.

Supplementary figure 7 The three largest families in the AGRE dataset. The colour of the filled symbols indicates the most probable class of the affected subjects under the optimal familial dependence LC model: red = class 1, yellow = class 5 and purple = class 7.

Supplementary figure 8 Correlation between SNPs with the strongest association signals detected in the AGRE sample at 6p24-p23. Correlation estimated in the HapMap CEU sample.

Supplementary figures

Supplementary figure 1.

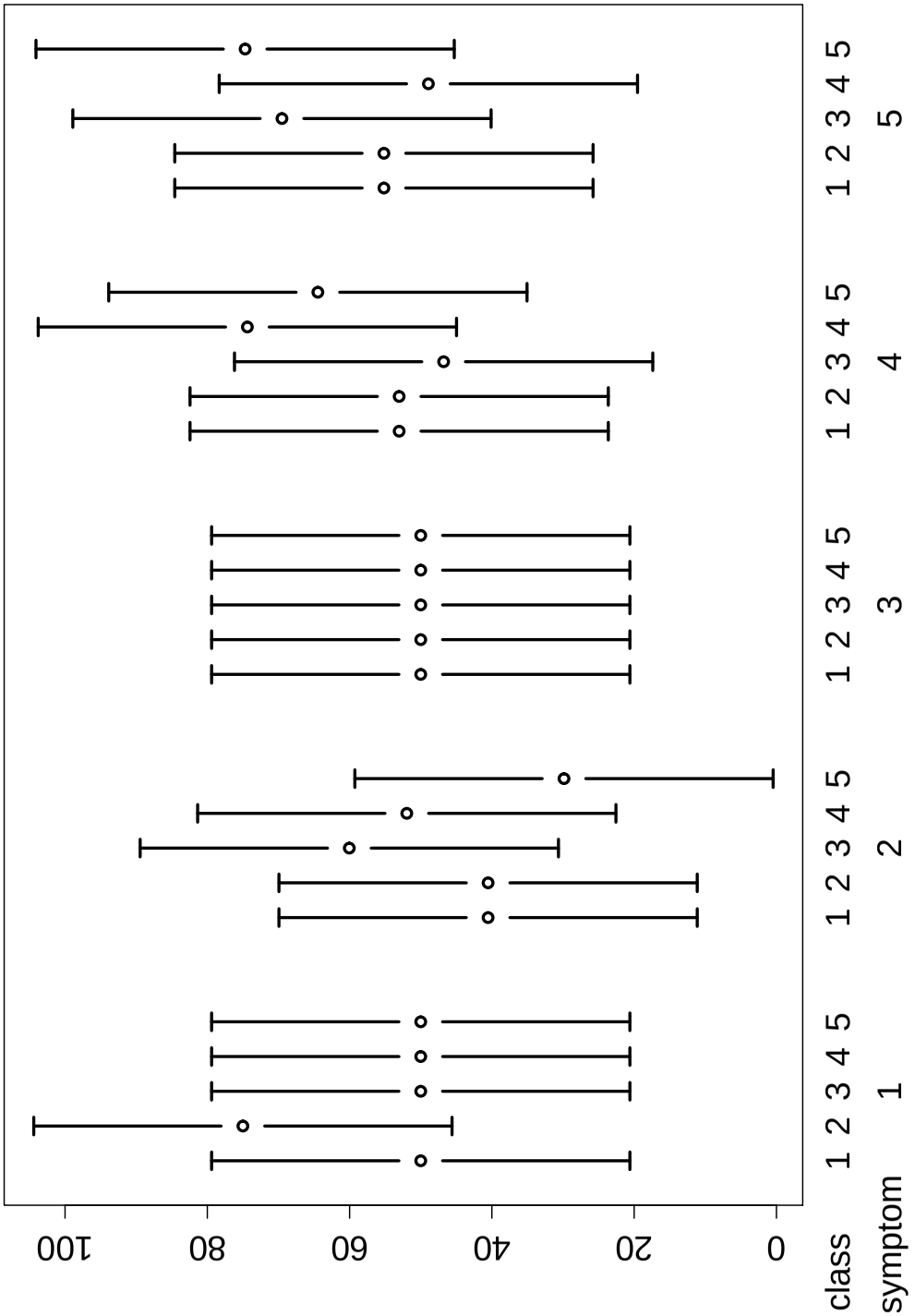

Supplementary figure 2.

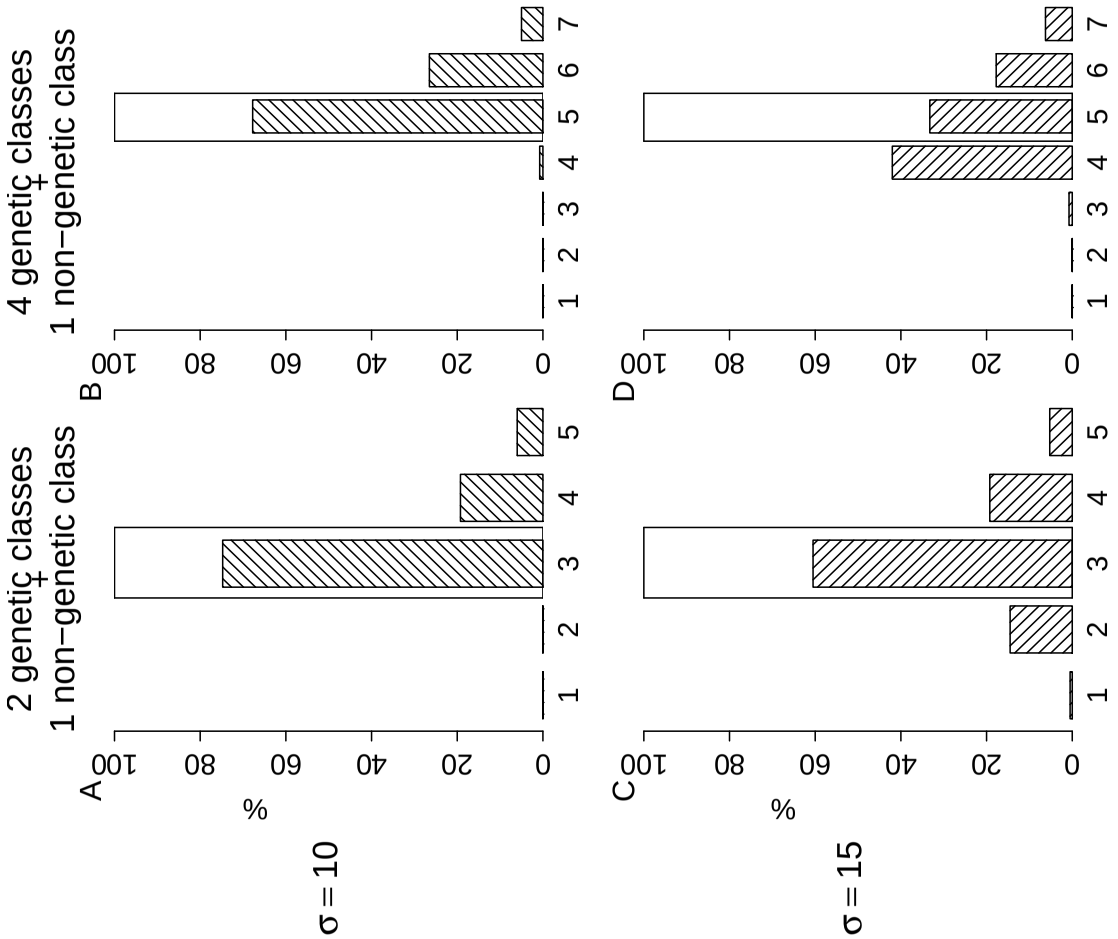

Supplementary figure 3.

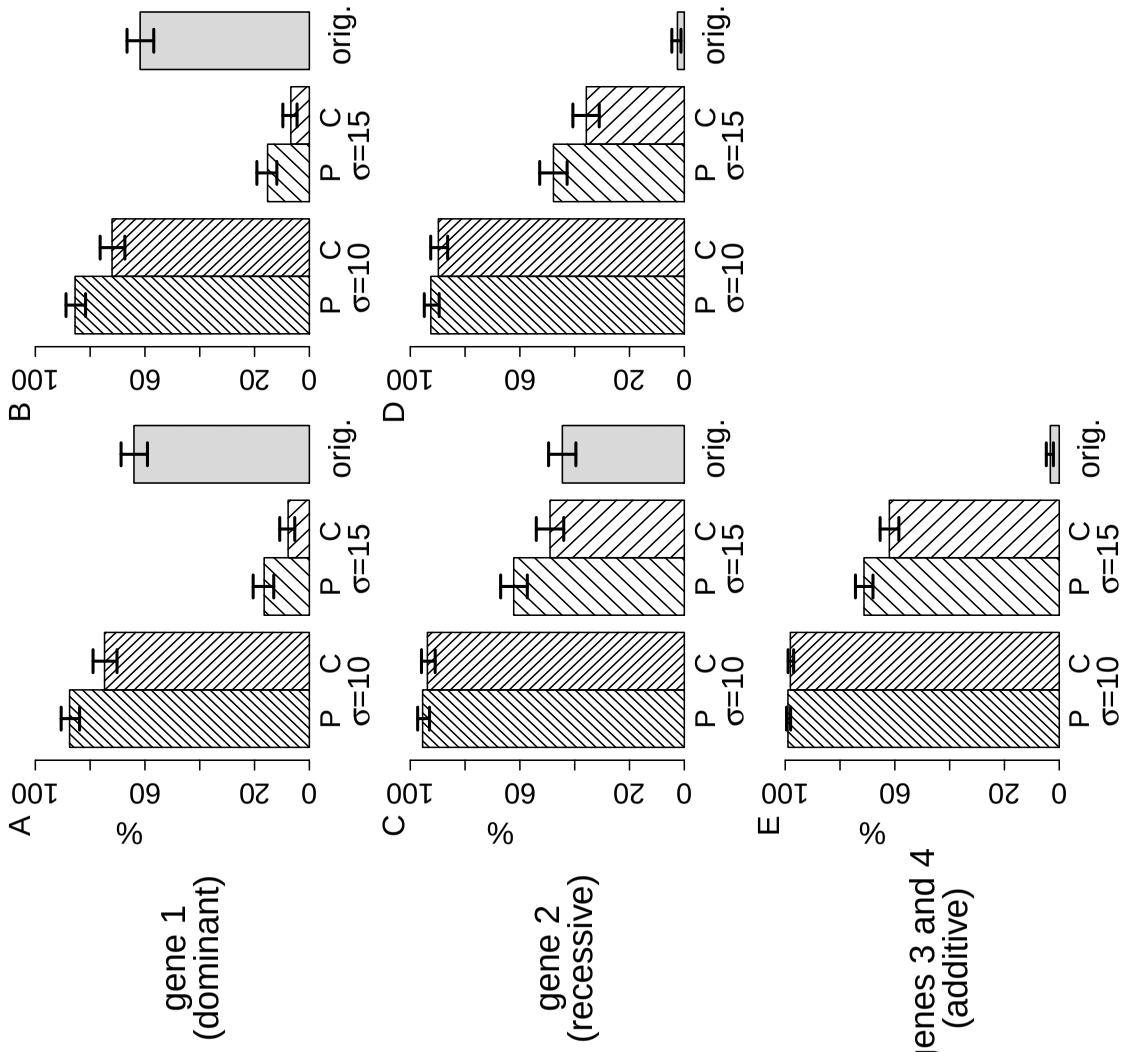

Supplementary figure 4.

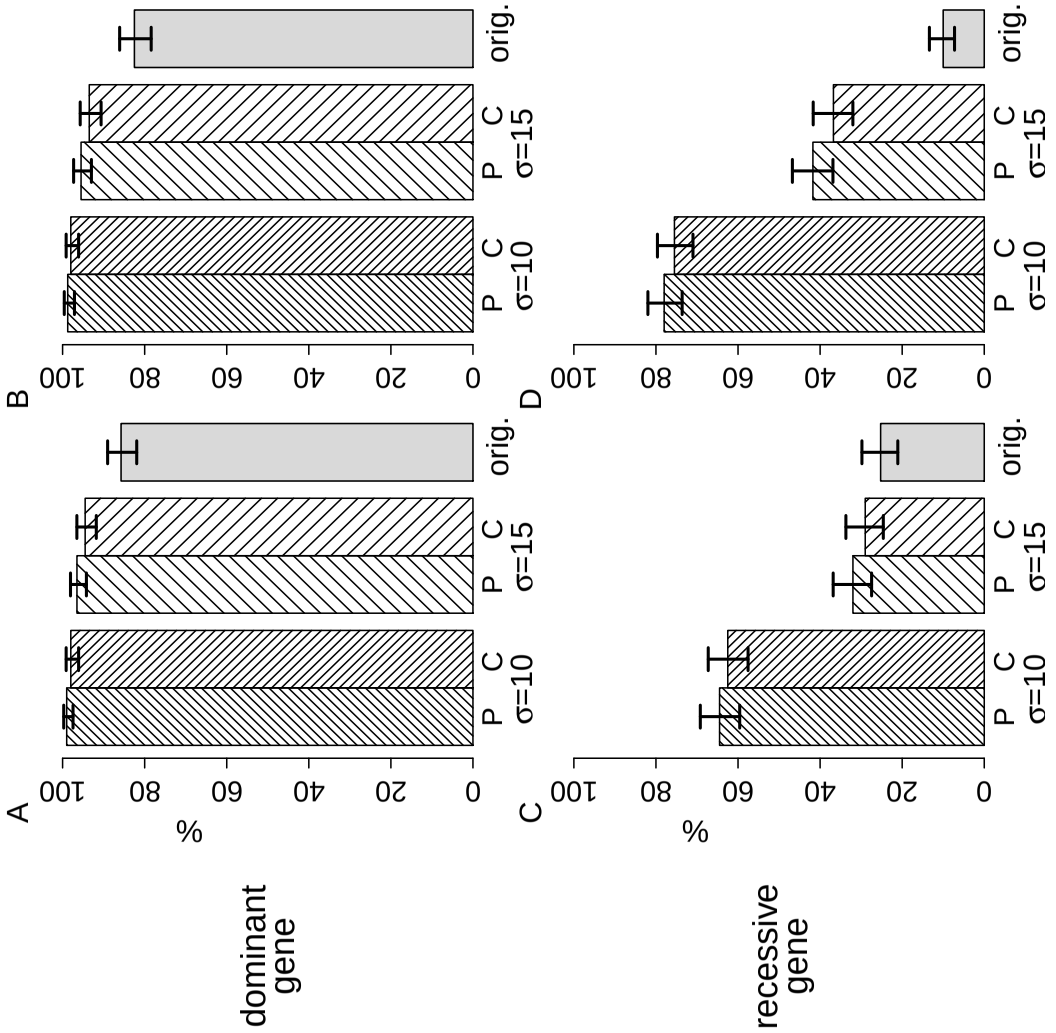

Supplementary figure 5.

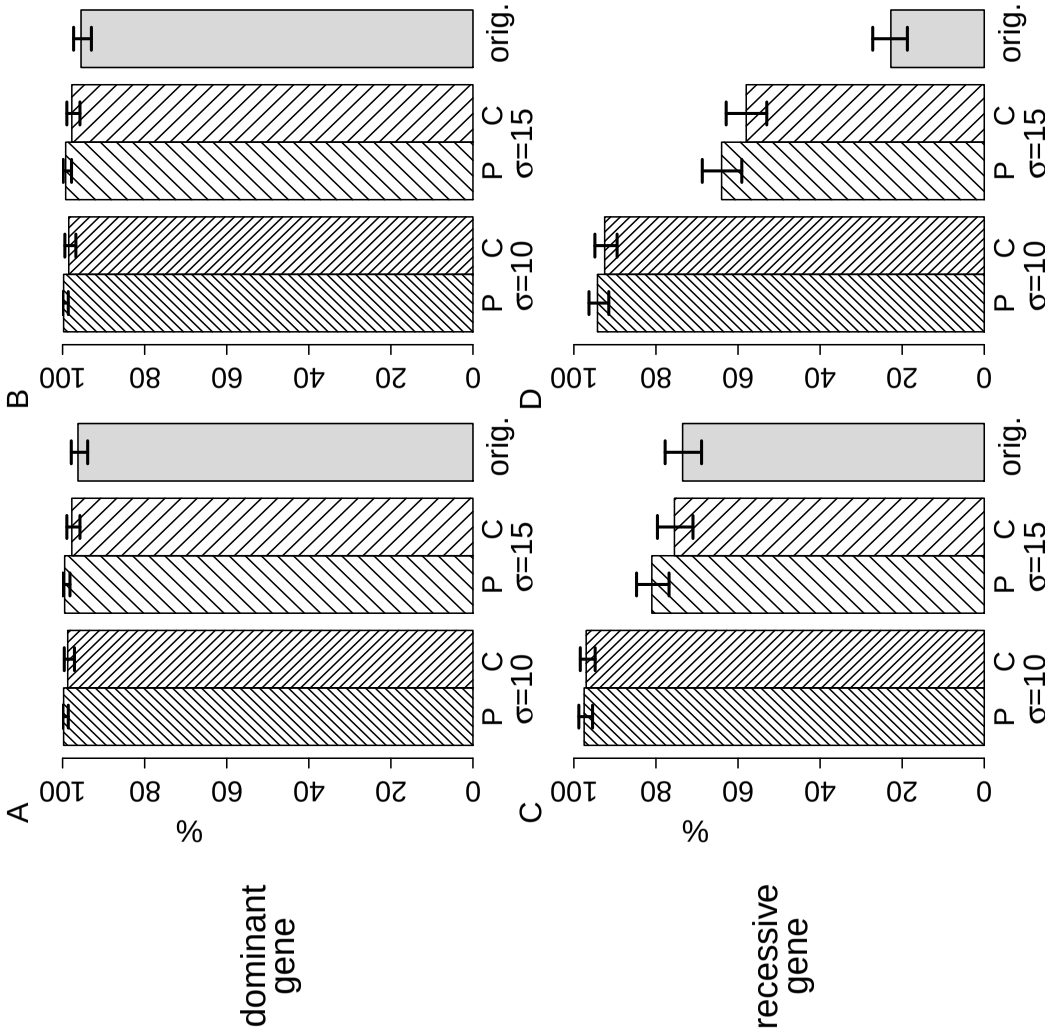

Supplementary figure 6.

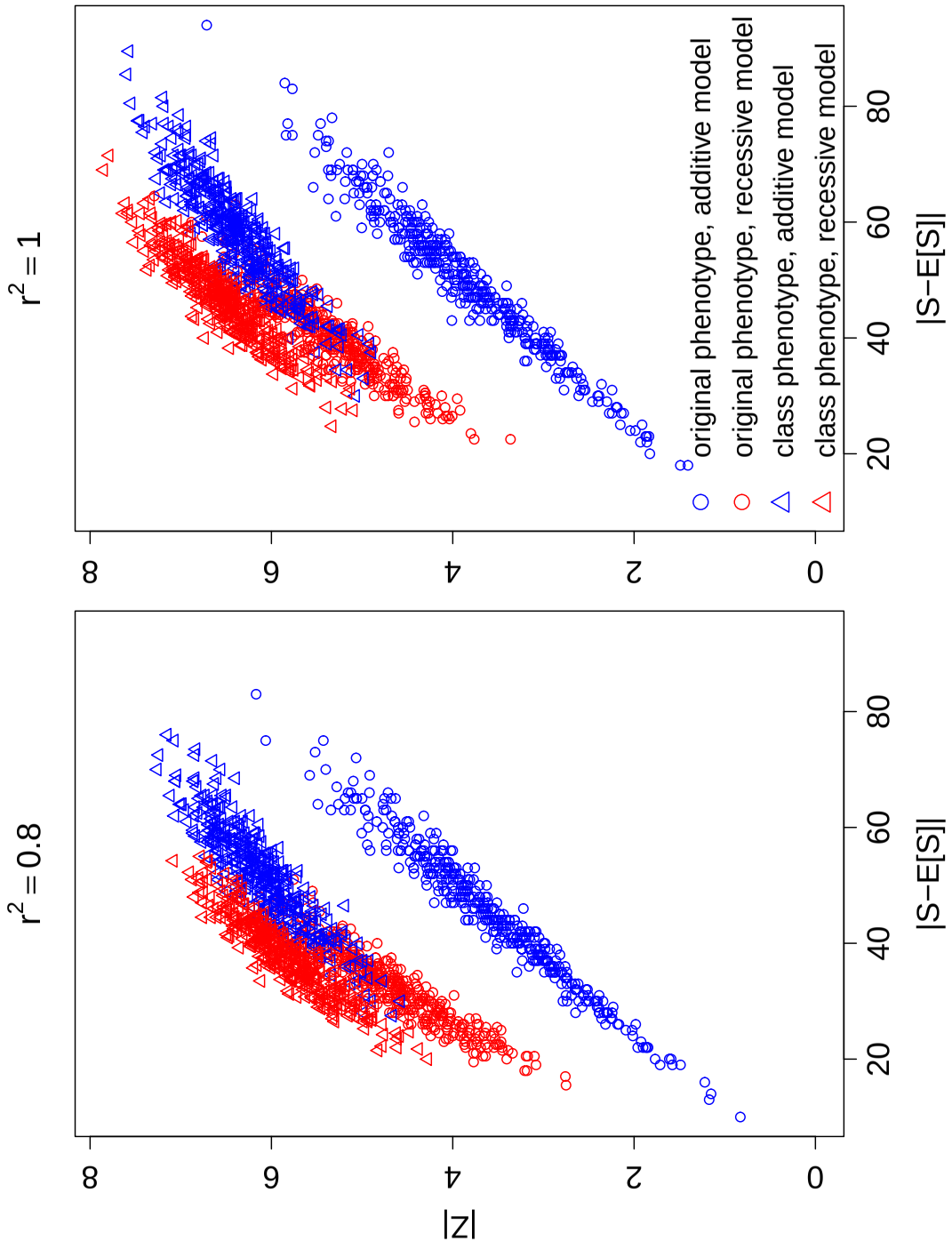

Supplementary figure 7.

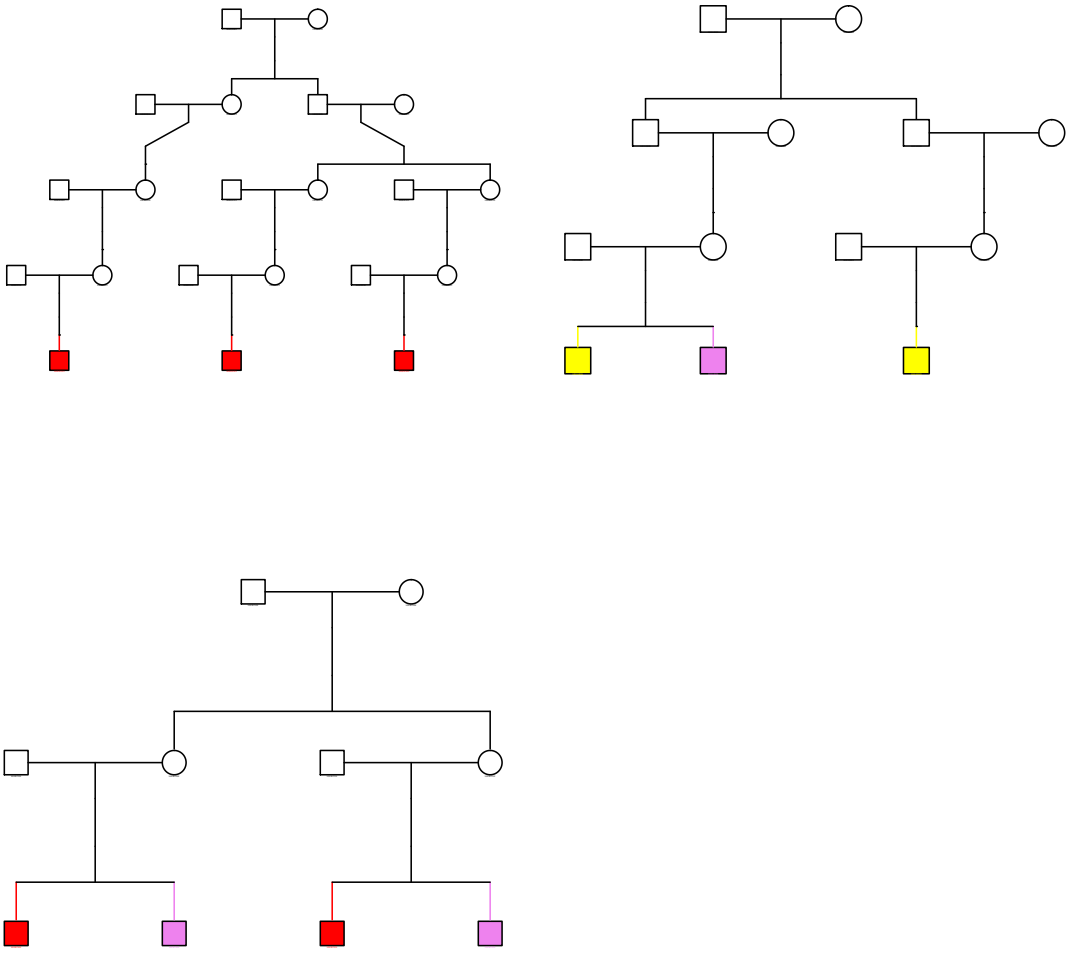

Supplementary figure 8.